ELSEVIER

Advances in Colloid and Interface Science 122 (2006) 79–91

ADVANCES IN COLLOID AND INTERFACE SCIENCE

www.elsevier.com/locate/cis

Modeling local flotation frequency in a turbulent flow field

Margaritis Kostoglou *, Thodoris D. Karapantsios, Kostas A. Matis

Division of Chemical Technology, Department of Chemistry, Aristotle University of Thessaloniki, University Box 116, 541 24 Thessaloniki, Greece

Available online 7 August 2006

Abstract

Despite the significance of turbulent fluid motion for enhancing the flotation rate in several industrial processes, there is no unified approach to the modeling of the flotation rate in a turbulent flow field. Appropriate modeling of the local flotation (bubble–particle attachment) rate is the basic constituent for global modeling and prediction of flotation equipment efficiency. Existing approaches for the local flotation rate are limited to specific set of conditions like high or low turbulence. In addition, the combined effects of buoyant bubble rise and/or particle gravity settling are usually ignored. The situation is even vaguer for the computation of collision and attachment efficiencies which are usually computed using the gravity induced velocities although the dominant mode of flotation is the turbulent one. The scope of this work is clear: the development of a general expression for the flotation rate in a turbulent flow field which will cover in a unified and consistent way all possible sets of the problem parameters. This is achieved by using concepts from statistical approach to homogeneous turbulence and gas kinetic theory.

Keywords: Flotation process; Mathematical modeling; Stochastic encounters; Turbulent flow field; Bubble–particle attachment frequency

Contents

1. Introduction

Flotation is a very complicated process combining fundamental hydrodynamics with many elementary physicochemical steps (bubble–particle interaction forces, particle–particle interaction forces etc.). As for other processes of chemical industry, modeling of flotation is an important step for better understanding the process itself and also a necessary tool for equipment design and optimization. Modeling of the particular process is a very difficult task not only due to the large number of involved phenomena but also due to the wide disparity of their size scales. The statement that flotation is "the encyclopedia of colloid science" (see [1]) is not enough to describe its

* Corresponding author. Tel.: +30 2310 99 7767; fax: +30 2310 99 7759.
E-mail address: kostoglu@chem.auth.gr (M. Kostoglou).

0001-8686/$ - see front matter © 2006 Elsevier B.V. All rights reserved.
doi:10.1016/j.cis.2006.06.014

complexity since phenomena like bubble–turbulence interaction (leading to particle scavenging) and two-phase flow hydrodynamics (bubbly flows), which are crucial for the flotation process, reside outside colloidal science interests.

This work attempts to develop a general framework for the modeling aspects of flotation in order to present with clarity not only the current situation but also the future requirements. A multiscale approach to the problem is necessary since the coexistence of size scales from the intra bubble–particle thin film (<1 μm) to the macroscopic equipment size (order of meters) renders a direct tackling procedure impossible. Even the well defined problem of a single phase flow is impossible to be solved simultaneously over all these size scales. The actual modeling problem is decomposed to the following size/procedural scales. The first scale (Scale I) is the macroscopic scale. It includes the motion (hydrodynamics) of the three phase (liquid–bubble–particle) mixture at the equipment size scale. The tools for studying this scale range from multiphase CFD codes ([2,3]) to conventional mixing models accompanied by experimental campaigns to assess the mixing characteristics of equipment ([4,5]). The second scale (Scale II) is the so-called mesoscopic one. In fact, this is not a distinct size scale but it refers to the procedure to transfer information from the particle microscopic scale to the equipment macroscopic scale through the appropriate descriptive equations. Mean field theories, such as the population balance equation [6], seem to be appropriate tools for this scale. The third scale (Scale III) is the microscopic one. This scale includes phenomena occurring at the bubble/particle size scale. The particle–bubble collision efficiency, attachment efficiency and particle–bubble aggregate stability are studied in this scale. Albeit hydrodynamic aspects at this scale can be in general modeled through a combination of first principles and statistical theories, modeling of the surface physicochemical aspects, which are equally important, is far more difficult. For this reason, they must be properly parameterized in a way that permits the experimental identification of undetermined parameters from relatively simple experiments. A complete model of a particular flotation process (industrial or in the laboratory) must include the above three scales.

Several scientific groups have been active over the last years in the subject of modeling the flotation process using different approaches and putting their attention at different size scales according to the above classification. Yoon and coworkers ([7–9]) are mainly (but not only) focused on the colloidal aspects of the flotation process. This group attempts to quantify directly the specific colloidal force (usual DLVO forces plus the so-called hydrophobic force) which determines the bubble–particle aggregation instead of using a lumped parameter, i.e. induction time, to account for this. Another very important contribution comes from Nguyen and his coworkers (e.g. [1,10]). The main focus of these authors is on the hydrodynamics of scale III. In addition, Nguyen has also studied extensively the stability of the film between a bubble and a particle as a separate sub-scale [1]. A very extensive discussion on the relation between film and bubble scale and the ways of their theoretical description can be found in [11]. Yet, another interesting contribution was made by King [12] who attempted to expand existing knowledge from scale III (with some modifications and improvements) to scale II. For instance, he showed how to tackle problems containing complications such as particle size distribution, particle composition distribution, distribution of induction times, etc. It is important to mention that the above authors are among the founders of the theory of flotation and their contribution to the subject is not restricted to the particular aspects examined here. A huge amount of work on scale III of flotation has been performed by Russian researchers (see Ref. [13]). The results of this work have been largely overlooked and many times rediscovered in the Western literature.

At this point it must be noted that the driving force for flotation is the relative motion between bubbles and particles. This can be of deterministic nature (buoyancy driven motion of bubbles and gravity settling of particles) or of stochastic nature (random motion due to a turbulent flow field). In the general case of an industrial flotation process, the two mechanisms coexist and this is the case we investigate in this work.

The approaches described above refer strictly to the case of deterministic driving forces for the bubble–particle collision. In practical applications, though, the stochastic driving force (induced by turbulent flow) is important and must be considered, too. A complete model (including all three scales) has been developed in a series of papers by Bloom and Heindel ([14–18]) in order to simulate a laboratory flotation deinking process. Both flotation mechanisms are taken into account by these authors but their scale II and scale I models are overly simplistic: a simple population balance is used for scale II and a completely mixed semi-batch reactor model is used for scale I. An also simple scale II model, based on population balances, is combined with a very detailed model of scale I, based on multiphase CFD codes, in the work of Koh and Schwarz ([2,3]). The drawback in the latter work is that only the turbulent flotation mechanism is considered invoking the high level of turbulence in the employed flotation equipment without, however, any numerical checking of this assumption.

Despite the abundant knowledge that has been accumulated over the years on the modeling of flotation, a generally accepted procedure has not yet been established. The purpose of the present paper is to set the basis for this by developing a theory for the computation of the "local" flotation rate (scale III) as general as possible which will incorporate the most acknowledged of the existing theories. This "local" flotation rate will be used in the future for the development of models for the other two scales (I and II).

The structure of the paper is the following: At first, the most recent models for bubble–particle collision and attachment efficiencies under deterministic conditions are reviewed and assessed in order to incorporate them in the general model to be developed. Then, the existing theories for the turbulent encounter rate are presented and their inconsistencies are pointed out. Composite laws for the turbulent rms (root mean square) velocity are derived next, that should be consistent with all turbulent encounter mechanisms at the corresponding limits. All the above approaches are unified using techniques from the kinetic theory of gases. Computational considerations of the proposed model are discussed next. Finally, the appropriate

models for the two efficiencies (collision and attachment) are chosen and several aspects of them regarding their contribution to the flotation frequency are extensively discussed.

2. Theory

The scope here is to develop an expression for the "local" particle–bubble aggregation rate under the influence of gravity and an arbitrary level of turbulence. To do this, we will start by reviewing the existing approaches, first for the case of deterministic collisions between a particle and a bubble and then for the more complicated and less studied case of stochastic turbulence induced collisions. The analysis here will be restricted to the case of inertialess particles and immobile (completely retarded) bubble surface. It is noted that only the most recent editions of the several existing approaches for the deterministic collisions will be examined. A detailed history and review of most of these approaches can be found in [1,11,13].

2.1. Deterministic encounters

The unit problem here is to find the frequency of aggregation between bubbles having a deterministic velocity U_b and radius R_b and particles having a deterministic velocity u_p (in the opposite direction) and radius R_p. According to well known considerations from the theory of colloidal particle aggregation, the aggregation (flotation) frequency (which can be transformed into rate by multiplication with bubble and particle concentrations) is given as:

$$K_d(R_b, R_p, U_b, u_p) = P\pi(R_b + R_p)^2(U_b + u_p) \tag{1}$$

where P is the fractional flotation efficiency i.e. the fraction of particles contained at the fluid volume that are scavenged by the bubble which will be permanently attached to the bubble. The efficiency P consists of two components i.e. $P=P_cP_a$. The first (P_c: collision efficiency) expresses the probability of one of the aforementioned particles to actually collide with the bubble (in the sense that only a thin liquid film separates the particle from the bubble after the impact). The second (P_a: attachment efficiency) expresses the probability of the collided particle to drain the thin liquid film and eventually aggregate with the bubble. According to the standard approach, the efficiency P_c is related to particle scale hydrodynamics whereas the efficiency P_a is related to the film scale hydrodynamics and particle–bubble physicochemical interactions.

The collision between a bubble and a particle is the result of a combination of the interception phenomenon (finite particle size) and the tendency of particles to deviate from fluid streamlines (due to their velocity u_p and/or their inertia). To calculate the collision efficiency, the fluid flow field around the bubble is needed and the way of computing it is a crucial part of the calculation of P_c.

The most recent theories for the computation of P_c and P_a are the following:

i) modification of the classical Yoon-Luttrell [19] approach by King [12], (henceforth model i).

The Reynolds number for the flow around a bubble (denoted as Re_b) is usually of an intermediate value between 1 and 100. This means that the analytical solutions for the flow field for $Re_b=0$ (Stokes flow) and for potential flow (good representation for large values of Re_b since then only the flow field towards the bubble contributes to the collision efficiency) cannot be used in realistic situations. But an analytical flow field is a prerequisite to obtain the efficiencies P_c and P_a in analytical form, as well. So, Yoon and Luttrell determined an analytical flow field for an arbitrary Re_b by interpolating between the above asymptotic analytical flow fields. The interpolation parameter was obtained by fitting the analytical flow field to published experimental data for the streamlines. Using their analytical flow field, Yoon and Luttrell [19] estimated P_c and P_a solely due to interception, in the limit of a small ratio R_p/R_b. The collision efficiency for combined interception and gravity and an arbitrary ratio R_p/R_b using the Yoon and Luttrell's flow field was provided by King [12]:

$$P_c = \left(1 + \frac{u_p}{U_b}\right)^{-1}\left[2\left(1 + \frac{R_p}{R_b}\right)^{-2} F(R_b + R_p) + \frac{u_p}{U_b}\right] \tag{2}$$

where

$$F(x) = \frac{1}{2}\left(\frac{x}{R_b}\right)^2 - \frac{3\alpha}{4}\frac{x}{R_b} + \left(\frac{3\alpha}{4} - \frac{1}{2}\right)\frac{R_b}{x} \tag{3}$$

$$\alpha = \exp\left(-\frac{4Re_b^{0.72}}{45}\,\frac{x/R_b - 1}{x/R_b}\right) \tag{4}$$

The parameter α used by King is not equal to the original one of Yoon and Luttrell which, however, can be restored by expanding the exponential term of Eq. (4) in a Taylor series and retaining only the first term (i.e. $x/R_b - 1 < 1$). It must be mentioned that the model of King refers only to the case of an immobile bubble surface (because the fluid flow profile corresponds to a zero slip velocity). The justification of this assumption is that due to the large amount of surfactants employed in practical flotation processes, bubbles behave (from a fluid dynamics point of view) as solid particles.

The attachment efficiency is computed as follows: First, the cumulative distribution of the residence time (sliding time in flotation language) of the particles on the bubble surface is computed. Then, the efficiency P_a is given as the fraction of the colliding particles having a sliding time larger than the induction time t_{ind}. The induction time is a parameter which collectively includes all physicochemical interactions between a bubble and a particle and must be determined experimentally or from empirical relations. The direct determination of the induction time by direct observation of the particle trajectories is very difficult especially for the case of relatively small particles for which the trajectory cannot be separated in two parts: one out of the bubble and another sliding on the bubble. In any case, the induction time is just a phenomenological parameter and it can be determined by fitting the above models to experimental attachment efficiencies. After some algebra, the following expression for the

attachment efficiency can be derived based on equations (9.20) and (9.27) of [12]:

$$P_a = 1 - \left[\frac{\exp\left(\frac{2(U_b^* + u_p)t_{ind}}{R_p + R_b}\right) - 1}{\exp\left(\frac{2(U_b^* + u_p)t_{ind}}{R_p + R_b}\right) + 1} \right]^2 \tag{5}$$

where

$$U_b^* = U_b \left[\frac{3}{2}\left(1 - \alpha + \alpha\left(\frac{R_p}{R_b}\right)^2\right) + \left(\frac{1}{2} - \frac{3\alpha}{4}\right)\left(\frac{R_p}{R_b}\right)^2 \right] \tag{5a}$$

ii) model developed by Bloom and Heindel (henceforth model ii)

Heindel and Bloom [15] also expanded the approach of Yoon and Luttrell [19] to account for particle settling and arbitrary size ratio R_p/R_b using the generalized flow field as given by Yoon and Luttrell. Their result for the collision efficiency is [15]:

$$P_c = \frac{1}{1+|G|}\left[\frac{(2L^3 + 3L^2)}{2(1+L)^3} + \frac{2}{15} Re_b^{0.72} \frac{(L^3 + 2L^2)}{(1+L)^4} \right] + \frac{|G|}{1+|G|} \tag{6}$$

where $G = -\dfrac{u_p}{U_b}$ and $L = \dfrac{R_p}{R_b}$.

A completely different approach from the usual one described above, has been followed by these authors for the derivation of the attachment efficiency [16]. A detailed analysis of the forces governing the sliding process of a particle on the surface of a bubble was provided. By including the resistive force due to film drainage, the gravitational force and the flow force between the bubble and the particle, the evolution equations for the thickness of the liquid film between bubble and particle were derived. After an extensive mathematical analysis, a closed form expression for the attachment efficiency was given:

$$P_a = \exp\left[-2\frac{\lambda}{C_B}\left(\frac{L}{1+L}\right)\left(\frac{g(L) - G}{|k(L)| - G}\right)(h_r - 1) \right] \tag{7}$$

where

$$g(L) = \left(1 - \frac{3}{4(1+L)} - \frac{1}{4(1+L)^3}\right) + \frac{Re_B^{0.72}}{15}\left(\frac{1}{1+L} + \frac{1}{(1+L)^3} - \frac{2}{(1+L)^4}\right)$$

$$k(L) = -\left[\left(1 - \frac{3}{2(1+L)} + \frac{1}{2(1+L)^3}\right) + \frac{2Re_B^{0.72}}{15}\left(\frac{1}{(1+L)^4} - \frac{1}{(1+L)^3} - \frac{1}{(1+L)^2} + \frac{1}{(1+L)}\right) \right]$$

λ is a measure of the deviation of the particle friction factor f_p from the Stokes flow i.e. $f_p = \lambda 6\pi\mu R_p$. For Stokesian particles (zero particle Reynolds number, Re_p) it is $\lambda = 1$. The empirical expression $\lambda = 1 + 0.216 Re_p^{1/2} + 0.0118 Re_p$ which is accurate for $0 < Re_p < 1000$ is used here [1]. According to this model, the bubble behaves at the bubble size scale as a solid particle so the employed flow field corresponds to an immobile bubble surface. On the other hand, at the scale of the bubble–particle film, the surface mobility of the bubble may be important so it influences the efficiency P_a through the parameter C_B. This parameter takes values between 1 (rigid surface) and 4 (fully mobile surface), depending on the degree of surface mobility.

In this model the well known induction time t_{ind} has been replaced by another parameter, h_r, which contains all the physicochemical features of the system. This parameter is the ratio of the initial thickness (at the moment of collision) of the bubble–particle liquid film to its thickness at the moment of disruption and formation of a particle–bubble aggregate. It is a purely empirical parameter and must be obtained (like t_{ind}) from experiments or empirical relations.

iii) model developed by Nguyen [20] (henceforth model iii)

There are two distinct shortcomings in the composite analytical flow field of [19]. First, it is derived by interpolation between two flow fields with fore and aft symmetry so it exhibits the same type of symmetry, too. But this symmetry is not actually obeyed by the real flow field. The collision angle (the maximum angle of attack on the bubble's surface where a particle can collide) is incorrectly assumed equal to $\pi/2$ invoking the fore and aft symmetry whereas the actual collision angle is smaller. This error in the collision angle can lead to a serious error in the collision and attachment efficiency computation. A second important weak point is that the Yoon and Luttrell flow field refers to the case of an isolated bubble. But in practical applications the volume fraction of bubbles (gas phase) in the liquid is finite, leading to a densification of liquid streamlines and hence to an increase of the flotation rate. Both the above drawbacks were overcome by Nguyen in an ingenious way. He solved numerically the Navier–Stokes equations around a bubble using a particle in "cell" approach (introduced in the context of flotation modeling in [21]) to account for the finite gas holdup. Then the fluid velocities were expanded in Taylor series with respect to variable $r/R_b - 1$ and the expansion coefficients up to the second order were obtained by employing asymptotic results and fitting the numerical solutions of the flow field for several values of R_b and gas holdup φ (for details see [22]). In this way, an approximate flow field valid in the region close to the bubble can be given in closed form as a function of bubble Reynolds number R_b and gas holdup φ. Using this flow field, the following relation for the collision efficiency due to interception and particle settling velocity was obtained:

$$P_c = \frac{1}{1+|G|}\left(\frac{R_p}{R_b}\right)^2 \frac{\sqrt{(X+C)^2 + 3Y^2} - (X+c)}{13.5Y^2} \times \left[\sqrt{(X+c)^2 + 3Y^2} + 2(X+c) \right]^2 \tag{8}$$

where

$$c = \frac{u_p}{U_b}\left(\frac{R_b}{R_p}\right)^2 \tag{8a}$$

$$X = \frac{3}{2}\left(1 + \frac{3Re_b/16}{1 + 0.309Re_b^{0.694}}\right) + (37.515 + 0.006Re_b^{1.367})\varphi \tag{8b}$$

$$Y = \frac{3Re_b/8}{1 + 0.217Re_b^{0.518}} + (0.466Re_b - 0.443Re_b^{0.96})\varphi \tag{8c}$$

The attachment efficiency is derived based on the concept of induction time but using the new flow field and taking into account the fact that the collision angle can be different than $\pi/2$. The final expression, after a transformation of trigonometric relations to algebraic for computational convenience, is

$$P_a = \left(\frac{1-p_a^2}{1-p_c^2}\right)\left(\frac{X + c + Yp_a}{X + c + Yp_c}\right) \tag{9}$$

where

$$p_c = \frac{\sqrt{(X+c)^2 + 3Y^2} - (X+c)}{3Y} \tag{9a}$$

and p_a is given from the solution of the following transcendental equation

$$\frac{(1-p_a)^{(1-B)/2}(1 + Bp_a)^B}{(1 + p_a)^{(1+B)/2}} = Z \tag{9b}$$

where

$$Z = \frac{(1-p_c)^{(1-B)/2}(1 + Bp_c)^B}{(1 + p_c)^{(1+B)/2}} \exp\left(-\frac{U_b(1-B^2)At_{ind}}{R_p + R_b}\right) \tag{9c}$$

$$A = \frac{u_p}{U_b} + \frac{R_p}{R_b}X + \left(\frac{R_p}{R_b}\right)^2 \frac{M}{2} \tag{9d}$$

$$B = \frac{R_p}{R_b}\frac{Y}{A} + \left(\frac{R_p}{R_b}\right)^2 \frac{N}{2A} \tag{9e}$$

X, Y have been already given in Eqs. (8b,c). M, N are functions of Re_b and φ:

$$M = -\frac{9}{2} - \frac{27Re_b}{32} + 0.4531Re_b^{1.1274} - (71.312 + 2.156Re_b^{0.954})\varphi^{1.367} - (370.374 + 44Re_b^{-212.032})\varphi^{1.912} \tag{9f}$$

$$N = -0.8748Re_b^{1.0562} + 7.65Re_b^{0.993}\varphi^{0.434} - 8.755Re_b^{0.982}\varphi^{0.618} \tag{9g}$$

The above relations were derived for the case of an immobile bubble surface. The corresponding relations for a fully mobile bubble surface were also derived in [23] but they are not given since they will be not used here. Nguyen also studied the effect of particle inertia to the collision and attachment efficiencies [1]. For the special case of small Stokes number, he was able to incorporate the inertia effect in closed form relations for P_c and P_a. Inertia effects will not be considered here since it can be shown that for the case of an immobile bubble surface and particle diameters smaller than 40 ìm they are not important. The contribution of inertia to the flotation rate defines the distinction between flotation and microflotation which is actually considered here [13]. An extensive analysis of the effect of the partial retardation (partially immobile bubble) to the flotation process can be found in [13]. The opposite to the present case (significant inertia, mobile bubble surface) has been studied extensively in [24] and [25].

2.2. Stochastic encounters

Despite the significance of stochastic (turbulence induced) encounters in practical flotation applications, this mode has not been studied from the modeling point of view at the same depth as the deterministic mode. In order to understand and quantify the influence of turbulence on the encounter rate between bubbles and particles, the phenomenological statistical theories of turbulence will be employed [26,27]. From this standpoint, turbulence induces encounters between suspended particles/bubbles in two distinct ways. Particles with size smaller than the smallest eddy of the flow field follow exactly the fluctuating local fluid velocity and this motion leads to encounters of first kind. The frequency of these encounters (turbulent mechanism I) is given as

$$K_{tI}(R_p, R_b) = 1.3(R_p + R_b)^3\left(\frac{\varepsilon}{\nu}\right)^{1/2} \tag{10}$$

where ε is the turbulent energy dissipation rate and ν is the kinematic viscosity of the fluid. The above expression has been derived for the first time by Saffman and Turner [28]. Latter, several other researchers used it with a different numerical constant in place of 1.3.

Particles of larger size (spanning several eddies) exhibit inertia with respect to turbulent flow fluctuations leading to a motion of particles different to that of the fluid. This motion constitutes the second mechanism of turbulent aggregation (turbulent mechanism II). The corresponding frequency was derived by Abrahamson [29] as

$$K_{tII}(R_p, R_b) = 5(R_p + R_b)^2\sqrt{u_{tp}^2 + U_{tb}^2} \tag{11}$$

where u_{tp}, U_{tb} are the roots of the mean values of the squares (rms) of the particle–fluid and bubble–fluid relative velocities, respectively. These velocities are given according to [30] as:

$$u_{tp} = \frac{0.685\varepsilon^{4/9}R_p^{7/9}}{\nu^{1/3}}\left(\frac{\rho_p - \rho_f}{\rho_f}\right)^{2/3} \tag{12a}$$

$$U_{tb} = \frac{0.685\varepsilon^{4/9}R_b^{7/9}}{\nu^{1/3}}\left(\frac{\rho_f - \rho_b}{\rho_f}\right)^{2/3} \tag{12b}$$

where ρ_p, ρ_b, ρ_f are the respective particle, bubble and fluid densities. The two turbulent flotation mechanisms (I and II) are usually considered to dominate at low and high turbulence intensity, respectively. The attempts to incorporate the collision and attachment efficiencies to a turbulent flotation model are very limited in literature. Recently, Koh and Swarz ([2,3]) used the efficiency functions of Yoon and Luttrell (derived for deterministic velocities) computed at the characteristic turbulent velocities given above (Eqs. (12a,b)), combined with the encounter frequency (Eq. (11)). Pyke et al. [31] used Eqs. (12a,b) for turbulent flotation (with coefficient 0.565 instead of 0.685) but they computed the efficiency functions using the deterministic velocities. These authors wonder about their approach and the combination of turbulent encounter model with deterministic efficiency functions as it is obvious in their characteristic phrase: "As far as we are aware, the literature is silent both experimentally and theoretically on these issues at present, so that there is a task defined for the future". Sherrell and Yoon [32] computed collision efficiencies in a turbulent flow field based on the energetic approach (comparison between kinetic and interaction energies). This approach is very different from the particle trajectories approach employed by the other researchers.

It is important to note that the turbulent inertia encounter mechanism should not be confused with the deterministic inertia encounter mechanism: the first one is a source of relative particle–bubble motion whereas the second one just enhances the deterministic collision efficiency by permitting particles to cross fluid streamlines around the bubble.

Eqs. (12a,b) were derived based on the balance between the inertial subrange acceleration and Allen's drag law. This balance may be appropriate at least for large bubbles (but with a constant value 0.83 instead of 0.685, according to [1]) but it cannot be used for particles. The appropriate balance for the particles is between dissipative subrange acceleration and Stokes drag law leading to ([1]):

$$u_{tp} = \frac{2\varepsilon R_p^3}{135\nu^2}\left(\frac{\rho_p - \rho_f}{\rho_f}\right)^{2/3} \tag{13}$$

The above relation can also be used for the case of small bubbles instead of Eq. (12b):

$$U_{tb} = \frac{2\varepsilon R_b^3}{135\nu^2}\left(\frac{\rho_f - \rho_b}{\rho_f}\right)^{2/3} \tag{13a}$$

2.3. Combined stochastic–deterministic encounters

The effect of the combined turbulent (mechanism II) and deterministic particle motion on the aggregation frequency has been addressed in [29]. Recently, Bloom and Heindel [17] rederived their final result for the particular application of flotation. The derivation was based on concepts and numerical integration techniques borrowed from the kinetic theory of gases. According to the latter authors, the frequency of encounters between bubbles and particles having deterministic velocities U_b and u_p and turbulent rms velocities U_{tb} and u_{tp} respectively, are:

$$K_{tII,d}(R_p, R_b) = 5(R_p + R_b)^2\sqrt{u_{tp}^2 + U_{tb}^2}\exp\left(-\frac{1}{2}\frac{(U_b + u_p)^2}{U_{bt}^2 + u_{pt}^2}\right) + \pi(R_p + R_b)^2\left(\frac{(U_b + u_p)^2 + U_{bt}^2 + u_{pt}^2}{U_b + u_p}\right) \times \mathrm{erf}\left(\frac{U_b + u_p}{\sqrt{2(U_{bt}^2 + u_{pt}^2)}}\right) \tag{14}$$

There is a subtle point in the above equation. In the case of zero turbulent velocities, the first term goes to zero and Eq. (14) degenerates to Eq. (1) as it should. For the case of zero deterministic velocities, the first term is equal to Eq. (11) and according to [29] and [17] the second term goes to zero based on the fact (as the above authors argue) that $\mathrm{erf}(x) \to 0$ faster than $x \to 0$. Yet, this is not true since the value of $\mathrm{erf}(x)/x$ in the limit $x \to 0$ is the finite number $2/\pi^{0.5}$. The correct asymptotic expansion of Eq. (14) in the limit of zero deterministic velocities leads to an equation similar to Eq. (11) but with a coefficient 7.5 instead of 5 (i.e. an error of 50%). This means that the integration performed in [29] is not correct.

The only attempt known to us to incorporate the collision and attachment efficiencies with deterministic and stochastic velocities to a unified model for the flotation rate was made by Bloom and Heindel [18]. They used Eq. (14) with their relations for the two efficiencies (Eqs. (6) and (7)) computed for the deterministic velocities. The drawback of the procedure is obvious: their efficiencies refer to deterministic velocities even in case where turbulent encounters dominate.

2.4. Towards a unified approach for flotation frequency

From the above it is apparent that despite the large amount of work devoted in developing expressions for the flotation rate, at this moment there is no consistent relation of flotation rate for bubbles with diameters 100–1000 μm, particles with diameters up to 40 μm, arbitrary intensity of turbulence and arbitrary gas holdup. The above expressions suffer from inconsistencies, errors in derivation or restricted domain of validity. Using a coherent approach, the existing theories need be corrected, assessed and selected in order to be merged in a unified expression for the flotation frequency.

The equation for the bubble turbulent rms velocity Eq. (12b) is valid only for large bubbles and high values of ε. As a result, it predicts unrealistically large values of bubble–fluid relative motion for small bubble sizes. Also, the exponent of ε is smaller in Eq. (12b) than in Eq. (10) which is a paradox since the turbulent encounter mechanism I refers to low turbulence intensity and mechanism II to high turbulent intensity. In order to get a general expression for the velocity U_{tb} valid for any bubble size and any turbulence intensity and leading to an encounter frequency smaller than that of turbulent mechanism I

as ε decreases, the harmonic average of the relevant expressions for the two regimes (inertia and dissipative sub-ranges of turbulence) is employed:

$$U_{\mathrm{tb}} = \left[\left(\frac{0.83\varepsilon^{4/9}R_{\mathrm{b}}^{7/9}}{\nu^{1/3}}\left(\frac{\rho_{\mathrm{f}}-\rho_{\mathrm{b}}}{\rho_{\mathrm{f}}}\right)^{2/3}\right)^{-1}+\left(\frac{2\varepsilon R_{\mathrm{b}}^{3}}{135\nu^{2}}\left(\frac{\rho_{\mathrm{f}}-\rho_{\mathrm{b}}}{\rho_{\mathrm{f}}}\right)\right)^{-1}\right]^{-1} \tag{15}$$

Eq. (10) can be obtained in several ways. Its derivation in [28] was based on the mean flux of fluid entering a sphere with radius $R_{\mathrm{p}}+R_{\mathrm{b}}$. The relative velocity of a bubble–particle pair follows the mean motion of fluid. An alternative derivation was based on the diffusion equation together with the appropriate expression for a spatially dependent turbulent diffusivity [33]. Fortunately, a third derivation procedure based on the kinetic theory of gases was proposed in [34]. In the latter, the stochastic quantities are not the relative particle/bubble–liquid velocities as in the case of mechanism II of turbulent encounters but the relative particle–bubble velocity. Since both modes of turbulent encounters can be described in terms of kinetic theory, this approach is appropriate to derive a composite law. The turbulent rms velocity for the relative particle–bubble velocity is given (employing a statistical approach to turbulence) as [28]:

$$W_{\mathrm{tr}} = (R_{\mathrm{p}}+R_{\mathrm{b}})\left(\frac{\varepsilon}{15\nu}\right)^{1/2} \tag{16a}$$

The above velocity refers to distances $R_{\mathrm{p}}+R_{\mathrm{b}}$ smaller than the microscale of turbulence and leads to the encounter rate given by Eq. (10). There is an additional inconsistency at this point. As the bubble radius increases, the velocity Eq. (16a) and the corresponding rate Eq. (10) increase without bounds leading to domination of the mechanism I encounters over the mechanism II encounters. But this behavior is unacceptable on physical grounds and it is due to the fact that the above velocity can be used only for relatively small bubbles. A generalization of the theory can be made by considering the structure factor of turbulence for the inertia regime (distance $R_{\mathrm{p}}+R_{\mathrm{b}}$ larger than the Kolmogorov microscale) and matching the resulting velocities from the two regimes at the bubble–particle distance equal to Kolmogorov microscale. Thus, the velocity W_{tr} is given by Eq. (16a) for $(R_{\mathrm{p}}+R_{\mathrm{b}}) \le \nu^{3/4}\ \varepsilon^{-1/4}$ and by

$$W_{\mathrm{tr}} = (R_{\mathrm{p}}+R_{\mathrm{b}})^{1/3}\varepsilon^{1/3}\left(\frac{1}{15}\right)^{1/2} \quad \text{for} \quad (R_{\mathrm{p}}+R_{\mathrm{b}}) > \nu^{3/4}\varepsilon^{-1/4} \tag{16b}$$

Up to this point, consistent expressions for the rms velocities of three processes have been derived. Namely these are: (1) bubble–liquid relative motion, (2) particle–liquid relative motion (both due to bubble/particle inertia) and (3) bubble–particle relative motion due to liquid small scale flow distribution. The three processes can be assumed independent from each other, so considering a normal distribution of velocity for each one of the three modes of motion and following the principles of kinetic theory leads to the following total frequency of turbulent encounters:

$$K_{\mathrm{t}} = \frac{\pi(R_{\mathrm{p}}+R_{\mathrm{b}})^{2}}{(2\pi)^{9/2}(U_{\mathrm{tb}}u_{\mathrm{tp}}W_{\mathrm{tr}})^{3}}\int\int\int\int\int_{-\infty}^{\infty}\int\int\int\int C \exp\left(-\frac{U_x^2+U_y^2+U_z^2}{2U_{\mathrm{tb}}^2}-\frac{u_x^2+u_y^2+u_z^2}{2u_{\mathrm{tp}}^2}-\frac{W_x^2+W_y^2+W_z^2}{2W_{\mathrm{tr}}^2}\right) \mathrm{d}U_x\mathrm{d}U_y\mathrm{d}U_z\mathrm{d}u_x\mathrm{d}u_y\mathrm{d}u_z\mathrm{d}W_x\mathrm{d}W_y\mathrm{d}W_z \tag{17}$$

where C is the total relative velocity between bubbles and particles computed as

$$C = [(U_x-u_x+W_x)^2+(U_y-u_y+W_y)^2+(U_z-u_z+W_z)^2]^{1/2} \tag{18}$$

Although at first sight the above expression seems complex, it takes only an integration over the velocity distribution functions of velocity C in order to find the average total bubble–particle relative velocity. To our knowledge, this expression is the most general one until now in literature for the frequency of turbulent encounters and it is the starting point for adding more mechanisms. The addition of the deterministic motion of bubbles and particles with velocities U_{b} and u_{p} (gravity induced motion has only z-components) can be made easily by proper modification of the velocity magnitude C:

$$C = [(U_x-u_x+W_x)^2+(U_y-u_y+W_y)^2+(U_z+U_b-u_z+u_p+W_z)^2]^{1/2} \tag{19}$$

Abrahamson [29] in his derivation modified the probability distribution of z-velocities, instead of the relative velocity C, to account for the deterministic motion. It can be shown that both approaches lead to the same results. On the other hand, Bloom and Heindel [17] modified both probability distributions and C, deriving an incorrect expression for the encounter frequency (their Eqs. (14), (21)–(23)). Strangely, their final closed form expression (their Eq. (24)) is the same with that of Abrahamson and does not correspond to their previously derived equations.

Eq. (17) is not amenable to analytical integration, so a numerical integration procedure is employed. But the numerical integration of a 9-fold integral is very cumbersome and a way for reducing the dimensionality must be found. The proposed procedure here is to permit some degree of correlation between the bubble–liquid and the bubble–particle modes of motion and to merge them in a single mode. The rms of this new combined mode of motion is given according to the laws of statistics as:

$$U_{\mathrm{cb}} = \sqrt{U_{\mathrm{tb}}^2+W_{\mathrm{tr}}^2} \tag{20}$$

This assumption reduces the 9-fold integration to a 6-fold one and makes the numerical computation of the encounter frequency manageable. Of course this assumption introduces an error which becomes larger as the ratio of the rms of the two merged variables gets closer to 1. It is very fortunate that in the present case the error of merging is negligible since the two

merged modes do not act simultaneously. For large bubbles U_{tb} is large whereas W_{tr} is very small and vice versa.

The next step is to incorporate the theories for collision and attachment efficiencies to the developed generalized framework for encounter frequency between bubble and particles. These efficiencies depend on the particle and bubble velocities as they approach to each other and it is not clear what value of these velocities corresponds to the general case considered here. Both deterministic and turbulent rms velocities have been proposed ([18,2] respectively) but a more general approach is needed. The kinetic theory decomposes the random encounter bubble–particle velocity to random events with deterministic velocities. But each event must have its collision and attachment efficiency corresponding to its particular velocities. In this way, the theories for attachment and collision efficiencies under deterministic encounter conditions can be incorporated to the kinetic theory approach and integrated over the velocities distributions to give the total flotation frequency.

The particle deterministic motion influences the two efficiencies in a different way than the bubble motion. This is due to the fact that the gravitational motion of a particle crosses the streamlines of the flow field created by the motion of a bubble. The reason for which W_{tr} is decided to merge with the bubble velocity U_{tp} and not with the particle velocity u_{tp} is that it corresponds to a liquid motion similar to that created by the bubble and not to a particle motion which can cross the liquid stream lines. This choice is critical for the correct evaluation of the collision and attachment efficiencies. The collision efficiency for the case of mechanism I is usually computed on the premise of an extensional flow field around the bubble ([35,36]) but the uniform flow field employed here permits a large degree of integration without sacrificing much accuracy. Summarizing all the above, the final expression for the composite flotation frequency is:

$$K_c = \frac{\pi(R_p+R_b)^2}{(2\pi)^3(U_{cb}u_{tp})^3}\int\int\int_{-\infty}^{\infty}\int\int PC \exp\left(-\frac{U_x^2+U_y^2+U_z^2}{2U_{cb}^2}-\frac{u_x^2+u_y^2+u_z^2}{2u_{tp}^2}\right) dU_x dU_y dU_z du_x du_y du_z \quad (21)$$

where

$$P = P_c([U_x^2+U_y^2+(U_z+U_b)^2]^{1/2},[u_x^2+u_y^2+(u_z-u_p)^2]^{1/2}) \times P_a([U_x^2+U_y^2+(U_z+U_b)^2]^{1/2},[u_x^2+u_y^2+(u_z-u_p)^2]^{1/2}) \quad (22)$$

$$C = [(U_x-u_x)^2+(U_y-u_y)^2+(U_z+U_b-(u_z-u_p))^2]^{1/2} \quad (23)$$

Anyone of the deterministic models presented in the previous sections can be employed for the computation of P_a and P_c.

2.5. Computational approach

The numerical computation of the integral in Eq. (21) is impossible by direct discretization techniques due to the large number of integration variables and their infinite range. A Monte Carlo integration approach is necessary. Even this approach converges very slowly for the particular type of integrand which takes values among several orders of magnitude. Fortunately, the type of integral in Eq. (21) is ideally suited for the easy application of an importance sampling technique instead of the slowly convergent random sampling [37]. The exponential term in the integrand in Eq. (21) is eliminated with the payoff to use normally deviating random numbers. The procedure is as follows: six velocities (U_x, U_y, U_z, u_x, u_y, u_z) are chosen from six normal distributions having zero mean and rms (U_{cb}, U_{cb}, U_{cb}, u_{tp}, u_{tp}, u_{tp}), respectively. The value of the product PC is computed for these random velocities. The procedure is repeated N_{MC} times for different sets of random velocities and the average value of PC is used for the computation of flotation frequency from $K_c=\pi(R_p+R_b)^2(PC)_{ave}$. The algorithm for random number generation following the normal distribution is taken from [38].

The above procedure can lead to the computation of flotation frequency with arbitrary accuracy but due to its stochastic nature and the large number of required computations it is not recommended for the estimation of the local flotation frequency in large scale flotation simulations. For this aim, approximate simpler expressions for computing K_c must be derived. The following approach is proposed here: At first, the bubble velocities U_x, U_y are merged to the new velocity U_{xy} and the particle velocities u_x, u_y are merged to the velocity u_{xy}. The procedure is the same as was applied to the merging of the bubble–liquid and bubble–particle modes of motion but at the present case the error can be much higher since the two merging components attain similar values. The rms of the new velocities are $U_{cb,xy}=2^{\beta}U_{cb}$ and $u_{tp,xy}=2^{\beta}u_{tp}$. The nominal value of β is 0.5 but since a highly approximating procedure has been applied, it is better to find β from fitting the approximate values of K_c to the exact ones. This is done by requiring the 4 dimensional and the 6 dimensional approaches to K_c (both computed via the Monte Carlo method) to yield the same value for zero deterministic velocities. The best choice is found to be β=0.65. Having reduced the dimension of integration to 4, the multidimensional Hermitte integration scheme (of order N_H) is employed which automatically takes into account the infinite integration domain and the exponential weighting functions.

$$\frac{K_{c,app}}{\pi(R_p+R_b)^2} = \pi^{-2}\sum_{i=1}^{N_H}\sum_{j=1}^{N_H}\sum_{k=1}^{N_H}\sum_{m=1}^{N_H} w_i w_j w_k w_m P_{c,ijkm} P_{a,ijkm} C_{ijkm} \quad (24)$$

where

$$P_{c,ijkm} = P_c([2h_i^2U_{cb,xy}^2+(\sqrt{2}h_jU_{cb}+U_b)^2]^{1/2},[2h_k^2u_{tp,xy}^2+(\sqrt{2}h_mu_{tp}+u_p)^2]^{1/2}) \quad (24a)$$

$$P_{a,ijkm} = P_a([2h_i^2U_{cb,xy}^2+(\sqrt{2}h_jU_{cb}+U_b)^2]^{1/2},[2h_k^2u_{tp,xy}^2+(\sqrt{2}h_mu_{tp}+u_p)^2]^{1/2}) \quad (24b)$$

$$C_{ijkm} = [(\sqrt{2}h_iU_{cb,xy}-\sqrt{2}h_ju_{tp,xy})^2+(\sqrt{2}h_kU_{cb}+U_b-(\sqrt{2}h_mu_{tp}-u_p))^2]^{1/2} \quad (24c)$$

where h_i and w_i (i=1,2,..N_H) are the Hermitte integration points and weights, respectively, which can be found in tabular form for several values of N_H (e.g. [39]).

The particle settling velocity is computed as [1]:

$$u_p = u_{p,Stokes}\left(1+\frac{Ar_p}{96}(1+0.079Ar_p^{0.749})^{-0.755}\right)^{-1} \quad (25)$$

where the Stokes settling velocity is given as

$$u_{p,Stokes} = \frac{2R_p^2(\rho_p-\rho_f)g}{9\mu}$$

and the particle Archimedes number Ar_p is given as

$$Ar_p = \frac{8R_p^3(\rho_p-\rho_f)\rho_f g}{\mu^2}$$

The bubble rising velocity is computed in a similar manner [1]:

$$U_b = U_{b,Stokes}\left(1+\frac{Ar_b}{96}(1+0.079Ar_b^{0.749})^{-0.755}\right)^{-1} \quad (26)$$

with $U_{b,Stokes} = \frac{2R_b^2\rho_f g}{9\mu}$ and $Ar_b = \frac{8R_b^3\rho_f^2 g}{\mu^2}$

This expression is derived assuming the bubble as a spherical solid particle and, therefore, is not of general validity. Nevertheless, for bubbles with a diameter smaller than 1000 μm (considered here) and for contaminated water it constitutes a very good approximation [1]. It is noted that the above velocity refers to an isolated bubble. The finite gas holdup must be taken into account as a correction to this velocity (e.g. via Richardson–Zaki index).

3. Results–discussion

The general expression for flotation frequency given by Eq. (21) includes all the earlier expressions for frequencies (isolated mechanisms) as asymptotic cases. For example, by setting the turbulent energy dissipation rate equal to zero, Eq. (21) is simplified to Eq. (1). In case of zero deterministic velocities, and with collision and attachment efficiencies equal to 1, Eq. (21) degenerates to Eq. (11) for large bubbles and high turbulent intensity or to Eq. (10) for very small bubbles and low turbulence intensity. Furthermore, for the expressions (10) and (11) it is assumed that the motion of both bubbles and particles obeys the same mechanism whereas the generalized Eq. (21) can account for the case of a bubble size corresponding to mechanism II and a particle size corresponding to mechanism I, a situation which prevails under practical conditions. The consistent incorporation of all the mechanisms in one composite expression is the major outcome and novelty of the present work.

3.1. Assessment of the collision and attachment efficiency submodels

Next, the question arises which of the three cited recent models (referred as i, ii, iii) for the efficiencies P_a and P_c should be used in Eq. (21). An assessment of these theories and comparison among their results is performed here in order to make the choice.

It is noted that according to model (iii), P_c increases with no bound as R_p/R_b increases. This is evidently wrong since the efficiency cannot become larger than unity. The reason for this inconsistency is that the model has been derived at the limit $R_p/R_b \ll 1$. In principle, this is not so bad since the whole theory for collision efficiency (assuming particles in a flow field induced by a bubble motion and separate handling of bubbles and particles) rely implicitly on this assumption. On the other hand, the derivation at the above limit leads model (iii) to have a large difference (of the order R_p/R_b) in the opposite direction compared with the other models even for values of the radii ratio as small as 0.1. Two sources of errors appear when it is attempted to use the model (iii) for larger values of the radii ratio. At first, the capture radius is R_p+R_b and not R_b as it has been assumed in the model's derivation. The error can be easily corrected by replacing R_b with R_p+R_b in Eqs. (8,8a). This modification is assumed to be part of the model (iii) in what follows. With this simple correction, the values of P_a are restricted between 0 and 1. The second source of error is the flow field which results from a near surface expansion. This means that although the employed flow field is indeed more accurate than the other models flow fields for $R_p/R_b \ll 1$, its accuracy diminishes as the ratio increases and gradually turns to be even less accurate from the flow fields used by the other models. Unfortunately, there is no easy way to correct the flow field as R_p/R_b increases.

In general, the collision efficiencies predicted by the three models are close to each other so in order to stress the differences, the ratios $P_{c,i}/P_{c,ii}$ and $P_{c,iii}/P_{c,ii}$ are shown in Fig. 1 versus particle diameter D_p (1–40 μm) for several bubble diameters D_b (between 100–1000 μm). In the calculations, the particle density is taken as ρ_p=2 gr/cm^3. The models (i), (ii) give the same P_c for D_b=100 and 300 μm (small Re_b number). As the bubble size and particle size increase the discrepancy between the two models increases (due to the different form of the fitting parameter α for the composite flow field they use) but it does not exceed 3% for the parameters studied here. The model (iii) in general is expected to predict smaller values of P_c than the other models since it takes into consideration the fact that the collision angle can be different than π/2. The expected behavior of the model is reasonable on physical grounds for small particle size

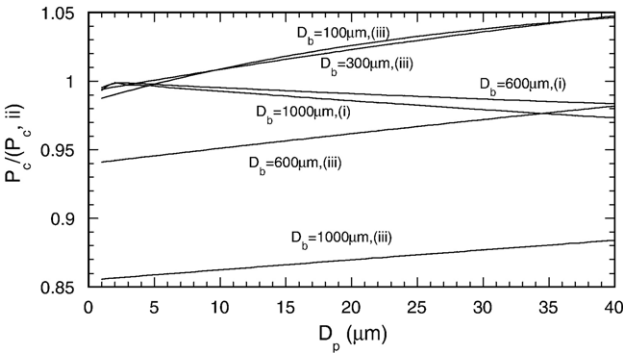

Fig. 1. Ratio between collision efficiency P_c from models (i) and (iii) to collision efficiency of model (ii) versus particle diameter D_p for several bubble sizes.

but the increase of $P_{c,iii}/P_{c,ii}$ as particle size increases is strange and may be due to the localized (near surface expansion) nature of the employed flow field. The only comparison known to us between any of the models presented here is the one performed in [15] between models (ii) and (iii). The curves P_c vs R_b from the two models are compared for a case having $R_p/R_b \ll 1$ for all R_b values. For small values of R_b, it is $P_{c,ii} > P_{c,iii}$ but the inequality is reversed as the bubble size increases. This behavior is fully compatible with the comparison shown in Fig. 1. The smaller values of P_c predicted by the model (iii) (due to a collision angle different than $\pi/2$) are essential to fit experimental results for collision efficiency (from [40]) which cannot be fitted accurately using the model (ii). In addition, model (iii) is the only one which takes into account the finite (non-zero) gas holdup. This is a crucial requirement since the local gas holdup in the flotation equipment is usually not zero so flotation frequencies derived for isolated bubbles cannot be used. The modified model (iii) is chosen for the calculation of P_c due to its important features of a finite gas holdup and a non $\pi/2$ collision angle. Nevertheless, a few percent error must be expected as the ratio R_p/R_b takes values larger than 0.1.

The next step is to assess the models for the attachment efficiency. Let us first compare the two models which have as fundamental parameter the induction time, t_{ind}. The attachment efficiency computed by the models (i) and (iii) are shown versus the induction time for two pairs of particle and bubble diameters in Fig. 2. As expected the attachment efficiency decreases as the induction time increases since the time spent by the particle on the bubble surface is not enough for permanent attachment. For small bubbles the Re_b is small and the actual flow field is close to exhibit a fore and aft symmetry. In this case the predictions of the two models for P_a are very close. However, for large bubbles ($D_b = 1000$ μm), the simplified flow field employed by model (i) is no more valid and the two models lead to very different results.

In order to assess the model (ii) and to check whether it is equivalent to the other models (i.e., is h_r just a function of t_{ind}?) or it exhibits a completely different behavior, the comparison of the predicted P_a among the three models versus D_b for $D_p = 10$ μm ($t_{ind} = 0.1$ *s*, $h_r = 1.98$) and $D_p = 30$ μm ($t_{ind} = 0.02$ *s*, $h_r = 1.45$) is shown in Fig. 3. Obviously, $P_{a,iii}$ decreases as bubble size increases due to the reasons already mentioned. The efficiencies for the two other methods show a smaller variation

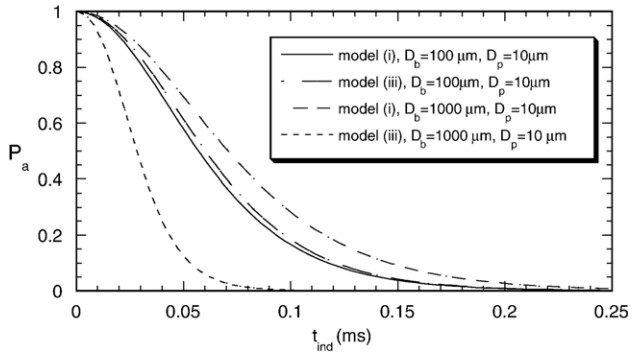

Fig. 2. Attachment efficiency P_a from models (i) and (iii) versus induction time t_{ind} for several pairs of bubble and particle diameters.

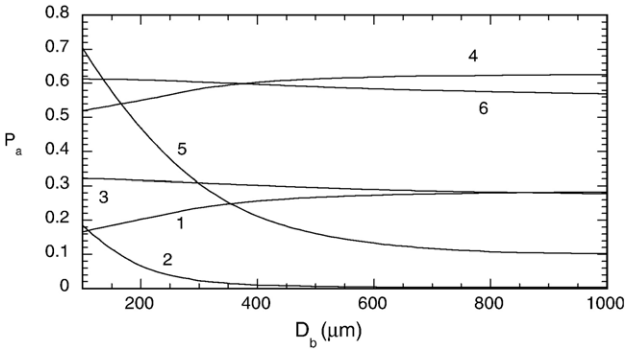

Fig. 3. Attachment efficiency versus bubble diameter D_b: (1)model (i), $t_{ind} = 0.1$ s, $D_p = 10$ μm (2) model (iii), $t_{ind} = 0.1$ s, $D_p = 10$ μm (3) model (ii), $h_r = 1.98$, $D_p = 10$ μm (4) model (i), $t_{ind} = 0.02$ s, $D_p = 30$ μm (5) model (iii), $t_{ind} = 0.02$ s, $D_p = 30$ μm (6) model (ii), $h_r = 1.45$, $D_p = 30$ μm.

(in opposite directions) but it is sure that the two methods cannot be assumed to be equivalent. So, the model (iii) which takes into account the disappearance of the fore and aft symmetry of the flow field as Re_b increases and leading to smaller attachment efficiencies must be used. It is noted that the dependence of the attachment efficiency on the bubble diameter shown in Fig. 3 is not a general feature but depends on the particular conditions. For example as the particle density increases this dependence disappears gradually leaving the attachment efficiency almost insensitive from D_b.

3.2. Analysis of the new unified flotation model

The consistency of the expressions used for the turbulent velocities will be presented through a simple example. The velocities (rms) U_{tb} (Eq. (15)) and W_{tr} (Eq. (16a)) are shown versus bubble diameter for the case $D_p = 10$ μm and three values of ε in Fig. 4. The anticipated behavior (not exhibited by previous models) that as D_b and ε increase, U_{tb} dominates over W_{tr} and vice versa is apparent. The particle inertia induced velocity u_{tp} range in this example from 1.85×10^{-5} m/s ($\varepsilon = 10$ m^2/s^3) to 1.85×10^{-7} m/s ($\varepsilon = 0.1$ m^2/s^3) and has insignificant contribution to the encounter rate.

The numerical aspects and requirements for the computation of flotation frequency will be examined next. The attachment

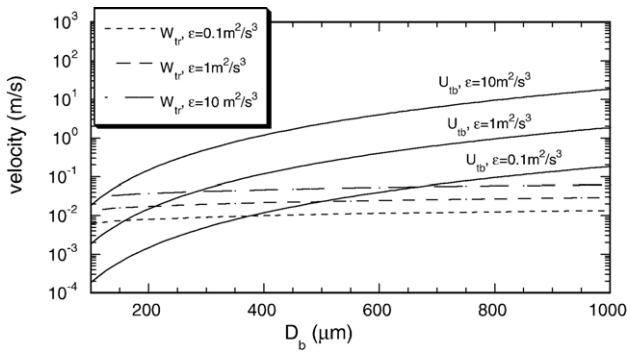

Fig. 4. Rms of relative bubble–fluid (U_{tb}) and bubble–particle (W_{tr}) turbulence induced velocities versus bubble diameter D_b for three values of turbulent energy dissipation rate ε ($D_p = 10$ μm).

efficiency model (iii) is somewhat more complicated than the other two as it requires the numerical solution of a transcendental equation for the cosine of the critical angle of attachment (p_a in Eq. (9b)). This is not a problem for isolated computations of P_a but for one computation of the flotation frequency via Eq. (21) the required numerical solutions of the algebraic Eq. (9b) are tenths of thousands so the stability and robustness of the solution method is very important. A method which seeks the solution in a specified interval is appropriate in this case. Here the bisection method is used utilizing the information that the critical angle of attachment is between zero and the collision angle (i.e. $p_c<p_a<1$). The computed value of the average generalized velocity $(PC)_{ave}$ (i.e., flotation frequency divided by $\pi(R_p+R_b)^2$) for the case $P=1$, $U_b=0$, $u_p=0$, $\varepsilon=1$ m^2/s^3, $\rho=2$ gr/cm^3, $R_p=5$ μm, $R_b=500$ μm is shown for several Monte Carlo realizations with several numbers N_{MC} of random points in Fig. 5(a). For this particular case (only turbulent encounters with $P=1$) the integration can be performed analytically to give $(PC)_{ave}=C_{ave}=0.3214$ m/s. This value is presented as a solid line in the Fig. 5(a) for reference. Apparently, as the number N_{MC} of computational points increases the exact solution is approached with a decreasing scatter around it. For $N_{MC}=40{,}000$ the error of a single simulation is no more than 0.5%.

Next, the same case but with taking into account the collision and attachment efficiency ($t_{ind}=0.006$ s) is considered and the corresponding values of $(PC)_{ave}$ are shown in Fig. 5(b). Now, there is no exact solution for reference but the convergence of the Monte Carlo method as N_{MC} increases is obvious. The fact that even with only 1000 Monte Carlo points, a rational approximation, ~3%, to the flotation frequency can be found is due to the sampling technique used. The number of points that would be needed for the same accuracy level using random sampling techniques would be at least an order of magnitude larger. It is important to note that as the deterministic velocities increase, the contribution of the stochastic part of the flotation frequency decreases so the Monte Carlo integration converges faster (i.e. the most demanding case is that of zero deterministic velocities examined above). Conclusively, a number $N_{MC}=40{,}000$ is in any case sufficient for the computation of flotation frequency.

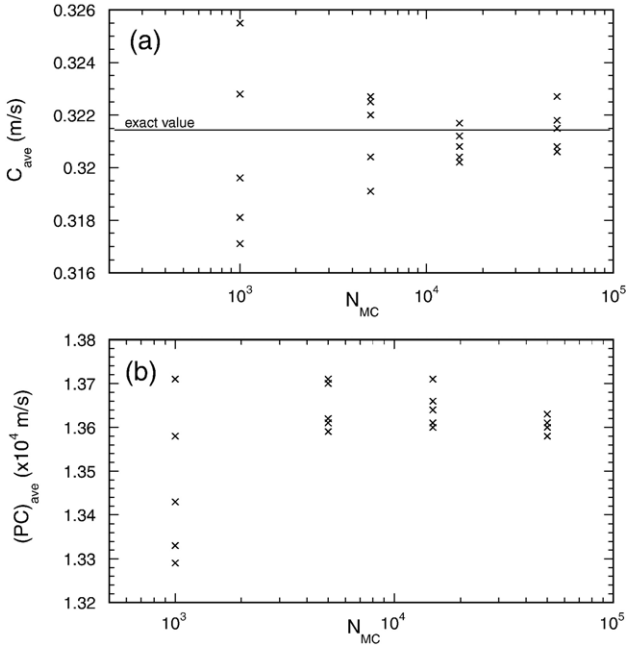

Fig. 5. Computed value of average total bubble–particle relative velocity C_{ave} for several Monte Carlo realizations with different number N_{MC} of computational points (a) ignoring efficiencies (b) including efficiencies (Parameters: $D_p=10$ μm, $D_b=1000$ μm, $U_b=0$, $u_p=0$, $\varepsilon=1$ m^2/s^3).

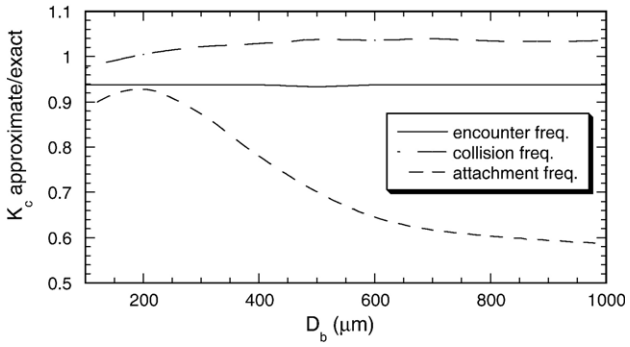

Fig. 6. Ratio between approximate (Eq. (24)) and exact (Eq. (21)) value of the encounter (i.e. $P=1$), collision (i.e. $P_a=1$) and attachment frequency K_c versus bubble diameter D_b. (Parameters: $D_p=10$ μm, $U_b=0$, $u_p=0$, $\varepsilon=1$ m^2/s^3).

The approximate relation (24) offers a deterministic way for the computation of flotation frequency. The number of terms N_H must be properly selected in order to keep within acceptable levels both computational load and accuracy. A rational choice $N_H=5$ leads to a total of 625 integration points. This level of computational cost permits the use of relation (24) for local flotation frequency in more demanding applications but the question about accuracy remains. To make the situation clear the ratio of the approximate (Eq. (24)) to the exact (Eq. (21)) encounter (i.e., $P=1$), collision (i.e., $P_a=1$) and attachment (for $t_{ind}=0.006$ s) frequencies for the system described above (for Fig. 5), is shown versus bubble diameter in Fig. 6.

The error in the encounter frequency is almost independent from D_b and it is the discretization error emerging from the attempt to approximate the function C in Eq. (21) in the interval $(-\infty,\infty)$ using just five collocation points (i.e. the error associated with the dimensionality reduction has been already eliminated by

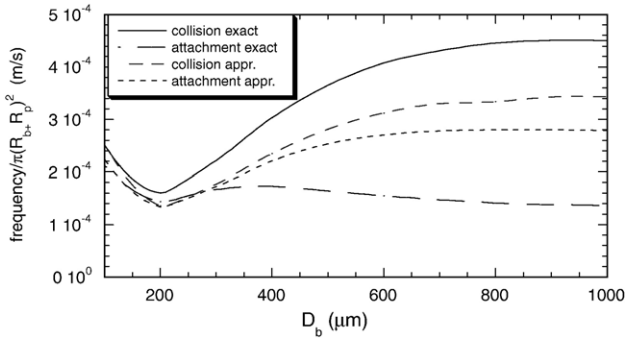

Fig. 7. Collision and attachment frequencies computed by Eq. (24) (exact) and by getting P out of the integral and computed it at the rms velocity values (approximate). (Parameters: $D_p=10$ μm, $U_b=0$, $u_p=0$, $\varepsilon=1$ m^2/s^3).

the proper choice of β). It is interesting that the approximation error for the collision frequency is smaller. This may be due to the fact that the function $P_c C$ is more uniform with respect to velocities than C, leading to larger integration accuracy. Finally, the attachment efficiency is a relatively sharp function of the velocities so the integration error in the attachment frequency computation can be quite large (up to 40% for the present example as shown in Fig. 6). A similar behavior is found for other sets of parameters. Keeping in mind again that the worst case (no deterministic velocities) for the approximate model has been examined here, the final suggestion is that the approximate flotation frequency expression (Eq. (24)) can be used but only for the case of hydrophobic particles (i.e. $t_{ind}=0$, $P_a=1$).

A basic feature of the model proposed here is that the efficiencies P_a, P_c are integrated over the velocity distributions instead of being computed at the turbulent velocity rms. To assess the quantitative differences between the two approaches, the corresponding collision and attachment frequencies for the system presented in the previous examples are shown in Fig. 7. The differences between the collision frequencies are in general small but the differences between the attachment frequencies are large enough to justify the computational effort needed by the approach proposed here. It must be noted that the approximation of computing the efficiency functions for a characteristic fluid velocity (including stochastic and deterministic contributions) with an analytical integration of the remaining terms would be a tempting alternative to be explored further but the analytical integration is not feasible. It must be recalled here that the integration performed in [29] is incorrect. The purpose of this work is the derivation of the expression for the flotation frequency in turbulent flow which covers (more or less) the region of particle diameter (2–40 μm) and bubble diameter 100–1000 μm and to propose procedures for its exact and approximate computation. Detailed parametric analysis of the model, incorporation of scale II models and comparison with experimental results will follow. Also, more accurate and simpler approximate expressions must be derived since practical applications may require several levels of additional integrations [12] (i.e. particle size distribution, bubble size distribution, induction time distribution, energy dissipation rate distribution).

It is noted here that the typical approach in flotation modeling literature is the incorporation of a model for particle detachment from the bubble, to the flotation frequency expression [1]. But according to the integrated approach proposed in the introduction, detachment cannot be assigned directly to the flotation (attachment) process. They are two separate processes which can occur individually. The incorporation of the detachment in the flotation rate is possible for modeling spatial homogeneous processes, but this is not so for other cases, e.g., for a region of a flotation equipment with high turbulent intensity and very small particle concentration. Obviously in this case, detachment may occur without attachment so the detachment rate cannot be considered just as a modifier of the flotation rate but it enters directly into the macroscopic balances as an individual process. The two phenomena of attachment and detachment will be combined in scale II (using our terminology) and not in scale I as it is the usual practice.

The unified model presented here is based on well known phenomenological theories on the structure of the turbulence and its effect on bubble–particle interaction. These theories of course are followed by a large list of assumptions some of which can be relaxed in the future. Any future modification/improvement of the partial theories (sub-models) can be directly incorporated to the proposed general model. Three special points will be discussed in what follows. As it has been already said the shape deformation of bubbles smaller than 1 mm moving by buoyancy is insignificant. But for high level of turbulence the turbulent acceleration may lead to the deformation of even smaller bubbles. This deformation must be taken into account to the theory of turbulent bubble–particle encounters for the case of high turbulence levels (mechanism II). A second point concerns the amount of turbulent energy accessible by each mechanism of stochastic bubble–particle relative motion. Whereas the whole turbulent energy is available for the mechanism I, it is very reasonable to consider that the energy of scales smaller than the bubble size does not contribute to the bubble acceleration (mechanism II). This issue needs further development but its incorporation in a CFD code using the present flotation frequency model is not an issue: The local turbulent energy dissipation rate given by the CFD will be used directly for the mechanism I rate but for mechanism II it will not be used directly but for the reconstruction of the local turbulent energy spectrum which will be integrated partially to give the amount of energy participating to the mechanism II. A third point is that the above theories do not take into account the effect of the existence of bubbles and particles in the structure of turbulence. This is not so significant since regarding mechanism I this effect actually is considered in two levels: the macroscopic effect is considered by the CFD codes and the bubble level effect is accounted through the consideration of the flow field around the bubble. As regards the mechanism II the effect of the existence of the third phase is not taken into account but it is not really important since the contribution of the turbulent inertia motion of particles (strongly influenced by the existence of the bubble) to the flotation rate is insignificant and the turbulent inertia motion of bubbles only slightly influenced by the existence of much smaller particles.

4. Conclusions

In the present work, a composite expression for the flotation frequency (frequency of successful bubble–particle collisions) in a combined gravitational and turbulent flow field is derived. For bubble and particle diameters in the ranges 100–1000 μm and 2–40 μm, respectively, the new expression incorporates most appraised earlier existing theories which, however, have a limited extent of validity and to which the new expression can degenerate as particular asymptotic cases. The particular processes taken into account is the settling and buoyancy motion of particles and bubbles, respectively, the bubble/particle–liquid relative motion due to bubble/particle inertia and its inability to follow the high frequency turbulent velocity fluctuation and the particle–bubble relative velocity due to the small scale structure of turbulence. In addition, the collision and attachment efficiencies are based on a flow field around the bubble which may

not exhibit fore and aft symmetry and take into account a finite gas holdup. Numerical methods for the exact and approximate computation of the composite flotation frequency have been developed and assessed. The proposed expression can be used for the computation of local flotation rates in simulating complex flotation process equipment.

References

[1] Nguyen AV, Schulze HJ. Colloidal science of flotation. New York: Marcel Dekker; 2004.
[2] Koh PTL, Schwarz MP. CFD modeling of bubble–particle collision rates and efficiencies in a flotation cell. Miner Eng 2003;16:1055–9.
[3] Koh PTL, Schwarz MP. CFD modeling of bubble–particle attachments in a flotation cell. Proceedings of centenary of flotation symposium, Brisbane, Australia, June; 2005. p. 201–7.
[4] Mavros P, Lazaridis NK, Matis KA. A study and modeling of liquid phase mixing in flotation column. Int J Miner Process 1989;26:1–16.
[5] Yianatos JB, Bergh LG, Diaz F, Rodriguez J. Mixing characteristics of industrial flotation equipment. Chem Eng Sci 2005;60:2273–82.
[6] Ramkrishna D. Population balances. Theory and application to particulate systems in engineering. San Diego: Academic Press; 2000.
[7] Yoon RH, Mao L. Application of extended DLVO theory, IV: derivation of flotation rate equation from first principles. J Colloid Interface Sci 1996;181:613–26.
[8] Mao L, Yoon RH. Predicting flotation rates using a rate equation derived from first principles. Int J Miner Process 1997;51:171–81.
[9] Yoon RH. The role of hydrodynamic and surface forces in bubble–particle interaction. Int J Miner Process 2000;58:129–43.
[10] Phan CM, Nguyen AV, Miller JD, Evans GM, Jameson GJ. Investigations of bubble–particle interactions. Int J Miner Process 2003;72:239–54.
[11] Ralston J, Dukhin SS, Mishchuk NA. Wetting film stability and flotation kinetics. Adv Colloid Interface Sci 2002;95:145–236.
[12] King RP. Modeling and simulation of mineral processing systems. London: Butterworth-Heinemann; 2001.
[13] Dukhin SS, Kretzschmar G, Miller R. Dynamics of adsorption at liquid interfaces, Studies in Interface Science, Series editors D. Mobius and R. Miller, Elsevier, Amsterdam; 1995.
[14] Bloom F, Heindel TJ. A theoretical model of flotation deinking efficiency. J Colloid Interface Sci 1997;190:182–97.
[15] Heindel TJ, Bloom F. Exact and approximate expressions for bubble–particle collision. J Colloid Interface Sci 1999;213:101–11.
[16] Bloom F, Heindel TJ. An approximate analytical expression for the probability of attachment by sliding. J Colloid Interface Sci 1999;218: 564–77.
[17] Bloom F, Heindel TJ. On the structure of collision and detachment frequencies in flotation models. Chem Eng Sci 2002;57:2467–73.
[18] Bloom F, Heindel TJ. Modeling flotation separation in a semi-batch process. Chem Eng Sci 2003;58:353–65.
[19] Yoon RH, Luttrell GH. The effect of bubble size on fine particle flotation. Miner Process Extr Metall Rev 1989;5:101–22.
[20] Nguyen AV. The collision between fine particles and single air bubbles in flotation. J Colloid Interface Sci 1994;162:123–8.
[21] Rulev NN, Derjaguin BV, Dukhin SS. Flotation kinetics of small particles by a group of bubbles. Kolloidn Z 1977;39:314–23.
[22] Nguyen AV. Hydrodynamics of liquid flows around air bubbles in flotation: a review. Int J Miner Process 1999;56:165–205.
[23] Nguyen AV. Particle–bubble encounter probability with mobile bubble surfaces. Int J Miner Process 1998;55:73–86.
[24] Dai Z, Dukhin S, Fornasiero D, Ralston J. The inertial hydrodynamic interaction of particles and rising bubbles with mobile surfaces. J Colloid Interface Sci 1998;197:275–92.
[25] Ralston J, Dukhin SS, Mishchuk NA. Inertial hydrodynamic particle–bubble interaction in flotation. Int J Miner Process 1999;56:207–56.
[26] Bachelor GK. The theory of homogeneous turbulence. London: Gambridge University Press; 1953.
[27] Baldyga J, Bourne JR. Turbulent mixing and chemical reactions. New York: Wiley; 1999.
[28] Saffman PG, Turner JS. On the collision of drops in turbulent clouds. J Fluid Mech 1956;1:16–30.
[29] Abrahamson J. Collision rates of small particles in a vigorously turbulent fluid. Chem Eng Sci 1975;30:1371–9.
[30] Schubert H, Bischofberger C. On the optimization of hydrodynamics in flotation processes. Proceedings 13th international mineral processing congress, Warsaw, vol. 2; 1979. p. 1261–85.
[31] Pyke B, Fornasiero D, Ralston J. Bubble particle heterocoagulation under turbulent conditions. J Colloid Interface Sci 2003;265:141–51.
[32] Sherrell I, Yoon RH. Development of a turbulent flotation model. Proceedings of centenary of flotation symposium, Brisbane, Australia, June; 2005. p. 611–8.
[33] Gruy F, Saint-Raymond H. Turbulent coagulation efficiency. J Colloid Interface Sci 1997;185:281–4.
[34] Yuu S. Collision rate of small particles in a homogeneous and isotropic turbulence. AIChE J 1984;30:802–7.
[35] Melis S, Verduyn M, Storti G, Morbidelli M, Baldyga J. Effect of fluid motion on the aggregation of small particles subject to interaction forces. AIChE J 1999;45:1383–93.
[36] Pnueli D, Gutfinger C, Fichman M. A turbulent-Brownian model for aerosol coagulation. Aerosol Sci Tech 1991;14:201–9.
[37] Elimelech M, Gregory J, Jia X, Williams R. Particle deposition and aggregation: measurement, modelling and simulation. London: Butterworth-Heinemann; 1995.
[38] Press W, Flannery B, Teukolski S, Vetterling W. Numerical recipes. The art of scientific computing 2nd edition. New York: Cambridge University Press; 1992.
[39] Scheid F. Numerical analysis. New York: McGraw Hill; 1968.
[40] Nguyen AV, Kmet S. Collision efficiency for fine mineral particles with single bubble in a countercurrent-flow regime. Int J Miner Process 1992;35:205–23.